

**Research Article***Open Access, Volume 2*

# Three-Dimensional Interactive Quantitative Surgical Planning with Complete Thoracoscopic Lateral Basal Segmentectomy

**Yun Liu<sup>1,2</sup>; Songlin Zhang<sup>1,2\*</sup>; Chaobing Liu<sup>1,2</sup>; Ming Yan<sup>1,2</sup>; Lailong Sun<sup>1,2</sup>**<sup>1</sup>Department of Cardiothoracic Surgery, The First College of Clinical Medical Science, China Three Gorges University, Yichang, China.<sup>2</sup>Department of Cardiothoracic Surgery, Yichang Central People's Hospital, Yichang, China.**Abstract**

**Objectives:** Thoracoscopic segmentectomy for the lateral basal segment (S9) is one of the most technically challenging anatomical segmentectomy. This study aimed to describe thoracoscopic segmentectomy of S9 or S9b using three-dimensional (3D) interactive quantitative surgical planning through inferior pulmonary ligament approach.

**Methods:** This retrospective study included 17 patients who underwent thoracoscopic S9 segmentectomy or S9b subsegmentectomy between February 2018 and December 2020. All procedures were performed using 3D interactive quantitative surgical planning through inferior pulmonary ligament approach.

**Results:** All procedures were successfully performed under thoracoscopic visualization, with no conversion to thoracotomy or lobectomy. The operation time of RS9 segmentectomy was significantly longer than that of LS9 segmentectomy ( $P < 0.01$ ). The operation time of S9 segmentectomy was significantly longer than that of S9b subsegmentectomy ( $P < 0.01$ ). Surgical resection margin ranged from 20.0 to 27.7 mm (median, 21.7 mm). Chest tube duration was 2 days (range 1-4 days) and postoperative hospital stay was 4 days (range 3-7 days). No postoperative morbidity and death were identified. Pathological examination revealed 7 cases of adenocarcinoma, 7 cases of minimally invasive adenocarcinoma (MIA), 2 cases of adenocarcinoma in situ (AIS), and 1 cases of atypical adenomatous hyperplasia (AAH). No recurrence or mortality was observed during the median follow-up period of 13 months (range, 1-34 months).

**Conclusions:** This is the first report of a cohort of patients undergoing S9 segmentectomy or S9b subsegmentectomy, 3D interactive quantitative surgical planning through inferior pulmonary ligament approach method for thoracoscopic S9 segmentectomy was feasible in our hands with acceptable safety and complications.

**Keywords:** Three-dimensional reconstruction; Lateral basal segmentectomy; Thoracoscopic; Inferior pulmonary ligament.

**Manuscript Information:** Received: Sep 06, 2022; Accepted: Sep 27, 2022; Published: Oct 06, 2022

**Correspondance:** Songlin Zhang, Department of Cardiothoracic Surgery, The First College of Clinical Medical Science, China Three Gorges University, No.183 Yiling Road, Yichang, Hubei, 443000, China. Tel: 86-717-6488482; Email: 278087836@qq.com

**Citation:** Liu Y, Zhang S, Liu C, Yan M, Sun L. Three-Dimensional Interactive Quantitative Surgical Planning with Complete Thoracoscopic Lateral Basal Segmentectomy. *J Surgery*. 2022; 2(2): 1057.

**Copyright:** © Zhang S 2022. Content published in the journal follows creative common attribution license.

## Introduction

The early diagnosis of lung cancer is becoming prevalent. Lung segmentectomy has become a common surgical procedure in thoracic surgery, which is increasingly being used for the treatment of early small-sized lung cancers [1-3]. However, anatomical segmentectomy is a much more complex procedure than lobectomy, and it's challenging and technique demanding, especially when performed under total thoracoscopic visualization. The main reason lies in the difficulty in dissecting the frequently variable segmental structures (vein, artery, and bronchus) and identifying the accurate intersegmental planes [4,5]. Furthermore, segmentectomy for S9 is one of the most challenging anatomical segmentectomy [6,7]. It is difficult to expose and correctly identify the target vessels and bronchus because they are commonly variable and deeply located in the lung parenchyma. Moreover, tailoring the intersegmental plane is also challenging in video-assisted thoracoscopic surgery (VATS) S9 segmentectomy [8]. 3D reconstruction images have the advantage of providing a clear identification of the pulmonary vessel branches even at the subsegmental and more peripheral levels, thus making this complicated surgery easier and more practical [9,10].

## Patients and methods

### Patients

All surgeries were performed by the same thoracic surgeon (Dr. Yun Liu) with assistant surgeons, who at least completed 200 cases of thoracoscopic anatomic lung resection per year. Between February 2018 and December 2020, 17 patients who underwent thoracoscopic S9 segmentectomy or S9b subsegmentectomy, all procedures were performed using 3D interactive quantitative surgical planning through inferior pulmonary ligament approach. All enrolled patients provided informed consent. The patients provided Informed Written Consent for the publication of their study data. The patients' preoperative characteristics and clinical outcomes were reviewed using a database of our institute. The study was conducted in accordance with the Declaration of Helsinki (as revised in 2013). The protocol of this study was approved by the institutional review board of Yichang Central People's Hospital (NO. HEC-KYJJ-2018-601-01) (2018-01-09).

### Selection criteria

The inclusion criterion for VATS segmentectomy in the present study was computed tomography (CT) indicating a single lesion around the lung (considered 1/3 outside the lung parenchyma) with a diameter of  $\leq 2$  cm and with at least one of the following: pathologically confirmed AIS, nodule with  $\geq 50\%$  ground-glass opacity (GGO) on high-resolution CT, and imaging-confirmed tumor doubling time of  $\geq 400$  days. Patients who are not suitable for lobectomy due to compromised cardiopulmonary function are also appropriate candidates.

### Preoperative planning

The preoperative workup of all patients included clinical history, physical examination, thin-slice CT of the chest, lung function test, heart function test, blood gas analysis, and basic examinations as usual. Brain magnetic resonance imaging, bone scintigraphy, or positron emission tomography/CT was also performed if necessary. Prior to the operation, the lesion location and anatomy

of the branches of the bronchus, arteries, and veins were identified using 3D reconstruction images. 3D reconstruction images were generated for all patients using the Materialise 3-Matic software (developed by Materialise Nv Co., Materialise's interactive medical image control system, Kingdom of Belgium. Serial number: A51D56D6-C3XE-0011-1F7605D216DF39D5). The distance from the lesion to the intersegmental plane was measured using 3D reconstruction images before the operation to ensure that the lesion was at least 2 cm away from the resection margin, and thus, the cut line was determined. The anatomic variations and positional relations of the basal segmental vessels and bronchi were analyzed. The location and radiological features of the target nodule was identified. Furthermore, the anatomic relationship between the nodule and the neighboring structures was collected to design an appropriate surgical excision (Figure 1).

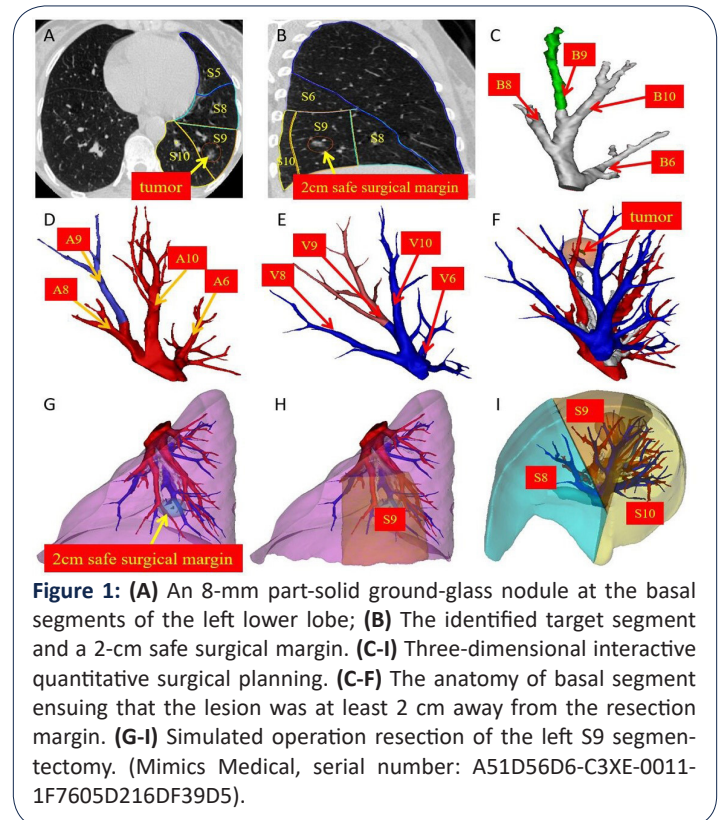


**Figure 1:** (A) An 8-mm part-solid ground-glass nodule at the basal segments of the left lower lobe; (B) The identified target segment and a 2-cm safe surgical margin. (C-I) Three-dimensional interactive quantitative surgical planning. (C-F) The anatomy of basal segment ensuring that the lesion was at least 2 cm away from the resection margin. (G-I) Simulated operation resection of the left S9 segmentectomy. (Mimics Medical, serial number: A51D56D6-C3XE-0011-1F7605D216DF39D5).

### Positioning, anesthesia and port placement

The patient was placed in the contralateral lateral decubitus position. General anesthesia was administered, and intubation was achieved through a double-lumen endobronchial tube, surgery was performed with the lung collapsed on the operating side. The surgeon stood at the dorsal side of the patient, and the assistant stood at the ventral side of the patient. The thoracoscope port (approximately 1.5 cm long) was placed at the midaxillary line of the 7th intercostal space. The main utility incision (approximately 3 cm long) was made in the 5th intercostal space at the anterior axillary line, whereas the assistant incision was located in the 8th intercostal space at the posterior axillary line (approximately 1.5 cm long). The incisions were protected with a silicone rubber wound protector (Figure 2).

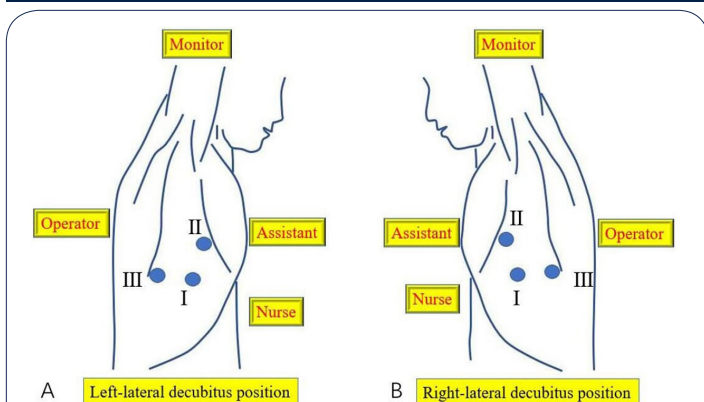


**Figure 2:** Arrangement of the surgical team and equipment. **(A)** For right-sided surgery, the patient is placed in a left-lateral decubitus position. **(B)** For left-sided surgery, the patient is placed in a right-lateral decubitus position. The main surgeon stood at the dorsal side of the patient, the assistant stood at the ventral side of the patient, and the nurse at the caudal side. Three ports are used: (I) The thoracoscope port (approximately 1.5cm long) was placed at the midaxillary line of the 7<sup>th</sup> intercostal space, (II) The main utility incision (approximately 3 cm long) was made in the 5<sup>th</sup> intercostal space at the anterior axillary line, (III) the assistant incision was located in the 8<sup>th</sup> intercostal space at the posterior axillary line (approximately 1.5 cm long).

### Surgical techniques

All procedures of segmentectomy were performed starting with an inferior pulmonary ligament approach and proceeding in a single-direction strategy without turnover of the lung repeatedly. The detailed procedures of RS9 and LS9 segmentectomy was similar, we took a LS9 segmentectomy as example to depict the detailed techniques in this study (Video 1).

**Video 1:** The detailed procedures of three-dimensional interactive quantitative surgical planning with complete thoracoscopic left lateral basal segmentectomy.

B9, bronchus of the lateral basal segment; A9, artery of the lateral basal segment; V9, vein of the lateral basal segment; S9, lateral basal segment; S10, posterior basal segment; S8, anterior basal segment; S6, superior segment.

The dissection was initiated from the inferior pulmonary ligament. The inferior pulmonary vein was cleared from the surrounding tissues, and its basal branches were dissected [8]. After a careful dissection, the branches of the inferior pulmonary vein to the target segment were skeletonized, this is the crux of the ensuing dissection. For the segmental veins, we should follow the principles of preserving uncertain veins, particularly the intersegmental veins. Corresponding to the 3D image, the name of each vein branch was determined and the internal segment vein V9a was divided. Sometimes, in order to ensure the safety of the margin, the intersegmental vein (V9b) between S9 and S10 should also be separated. After the V9 was severed, we dissected the lower lobe bronchus. The stem of the basal segmental bronchus was dissected. The bronchial branches were further dissected along the stems from proximal to distal [8]. B9 consists of B9a and B9b, B9 itself is usually very short before bifurcation into B9a and B9b, and the angle between these two subsegment bronchi is often estimated to be close to 90 degrees, the stem and branches of B9 were usually dissected from proximal to distal along the stems. B9b was more comfortable to take since it was located

in the shallow and more accessible hilar structures from this approach, B9a was less accessible as its location was much deep. Therefore, it is sometimes difficult to isolate the B9 trunk. We have to deal with B9a and B9b respectively, B9b was severed first and B9a was severed later, the stem and branches of the common basal segmental bronchus were usually dissected from proximal to distal along the stems, at the same time peri-bronchial lymph nodes were retrieved. Sometimes, if B9a was very close to B9b, we just need to deal with B9, corresponding to the 3D image, the B9 was confirmed and severed. After the bronchial branch was severed, the target segmental feeding artery always came into sight directly because it was always running along the bronchus. The last step was managing the intersegmental plane and dividing the lung parenchyma. A modified inflation-deflation method was used to identify the intersegmental plane [11]. After the targeted segment structures were dissected, the collapsed lung was initiated to fully re-expand with controlled airway pressure under 20 cm H<sub>2</sub>O, followed by single lung ventilation. After an interval of approximately 15 min, an irregularly curved demarcation was identified naturally between the deflated preserving segments and the inflated target segment. Furthermore, the contour of the target segment was displayed. Thereafter, staple-based 3D tailoring was performed. For the management of the intersegmental plane, we started from the relatively thin part of the lung tissue and gradually reached the segmental gate and the thick part of the lung. The specific steps were as follows: the first step was opening the boundary between S8 and S9, the second step was opening the boundary between S8 and S9 along the straight line where the lower lung ligament is located, the third step was opening the boundary between S9 and S10, and the last step was opening the boundary between S6 and S9. The use of a stapler for cutting the intersegmental plane does not affect the expansion of the residual lung and does not cause atelectasis (Figure 3).

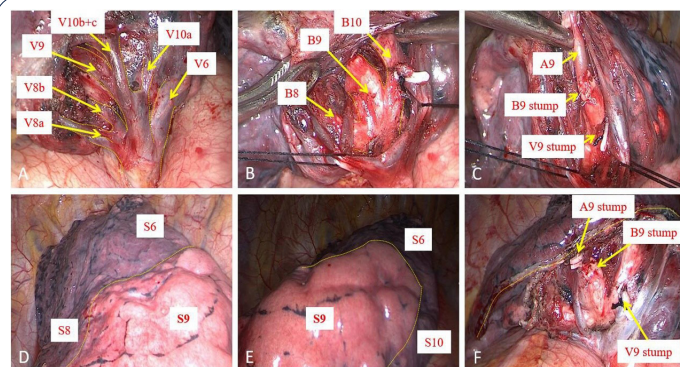


**Figure 3:** **(A)** Manage the inferior pulmonary vein, identifying the intersegmental vein V8b and V9. **(B)** Manage the bronchus, identifying B9. **(C)** Manage the artery. The artery generally corresponded to the bronchus one by one and slightly deviated from the spine. After the bronchial branch was severed, the A9 artery was observed. **(D,E)** Managing the intersegmental plane and dividing the lung parenchyma. The inflation-deflation approach was used to identify the intersegmental plane; the contour of the target segment was displayed. **(F)** View of the hilum following LS9 removal showed the stumps of the targeted bronchi and vessels.

Pathological examination of the frozen section confirmed the presence of a minimally invasive adenocarcinoma. The hilar and mediastinal lymph nodes were obtained and sampled. The view of the hilum following LS9 removal showed the stumps of the targeted bronchi and vessels. The surgical margin width was >20 mm. Finally, the lung was dilated and air leakage was tested from the stump of the bronchus and the resection margin of the lung. An 8F thoracic catheter connected to a negative pressure drainage bottle was placed in the observation hole. The operative time was 102 minutes, with an estimated blood loss of 35 ml. Early mobilization out of bed was started 12h postoperatively. The chest tube was removed on postoperative day 3, the postoperative hospitalization time was 4 days, and the final pathology revealed the presence of a pTmi1N0M0 minimally invasive adenocarcinoma. At 3 months after the operation, the patient underwent chest CT examination, revealing the presence of a well inflated lung (Figure 4).

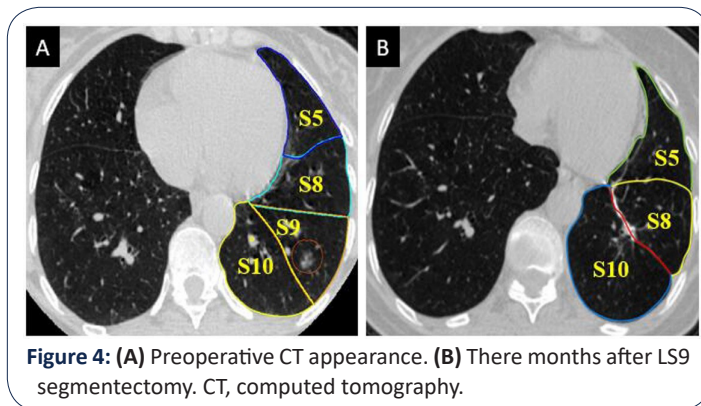


**Figure 4:** (A) Preoperative CT appearance. (B) Three months after LS9 segmentectomy. CT, computed tomography.

The aforementioned techniques were used for most cases of single or combined basal segmentectomy without considering the interlobar fissure was complete or not. Margins were an important consideration for segmentectomy, the specimen must be examined after resection, surgical margin was checked immediately. The surgical margin was sent for intraoperative frozen section pathological examinations, if the surgical margin was insufficient, an additional wedge resection would be performed. The chest tube was removed if there was no air leak, well inflated lung on chest X-ray, and less than 150 ml of drainage during the latest 24 hours. In cases with pulmonary adenocarcinoma, the new proposed histologic classification system<sup>18</sup> and the eighth edition of TNM staging system<sup>19</sup> were adopted for histologic typing and surgical-pathologic staging, respectively.

### Statistical analysis

The data were analyzed using SPSS, version 22.0 (SPSS Inc., Chicago, IL, USA). Quantitative variables were expressed as median and range.

### Results

Patients' characteristics are shown in (Table 1). The study group included 5 (29.4%) men and 12 (70.6%) women, ranging in age from 26 to 71 years (median, 57 y). Among these, 2 cases were active smokers. Regarding all patients, body mass index ranged from 20.2 to 25.1 (median, 22.7) and lesion diameter ranged from 8 to 17 mm (median, 13.7 mm), with 7 (41.2%) lesions having pure GGO, the consolidation ratio of 10 (58.8%) lesions was <50%, surgical resection margin ranged from 20.0 to 27.7 mm (median,

21.7 mm). Eight patients underwent right segmentectomy (five RS9 segmentectomy and three RS9b subsegmentectomy) while nine patients underwent left segmentectomy (seven LS9 segmentectomy and two LS9b subsegmentectomy). 3D reconstruction was successful in all patients, facilitating determination of the operation plan according to simulation results; adequate resection margin distance was found for all patients. All procedures were successfully performed under thoracoscopic visualization, with no conversion to thoracotomy or lobectomy. In this group of patients, pathological examination showed that curative resections were achieved with free surgical margins in all patients. All patients had an R0 complete cancer resection on histology. The histological subtypes of the segmental lesions included 7 of adenocarcinoma, 7 cases of MIA, 2 cases of AIS, and 1 case of AAH. Among patients with AIS or MIA, systemic hilar and mediastinal lymph node sampling was performed in 9 patients. Systemic hilar and mediastinal lymph node dissection were performed in 7 patients among those with adenocarcinoma. No patients were identified with postoperative lymph node involvement. The pathological examination characteristics of the patients are shown in Table 2. The median operation time of thoracoscopic left S9 (LS9) segmentectomy was 122 min (range, 67-171 min), the median operation time of thoracoscopic right S9 (RS9) segmentectomy was 156 min (range, 75-217 min), the operation time of RS9 segmentectomy was significantly longer than that of LS9 segmentectomy ( $P < 0.01$ ). The median operation time of thoracoscopic S9b subsegmentectomy was 101 min (range, 67-131 min), the median operation time of thoracoscopic S9 segmentectomy was 167 min (range, 79-217 min), the operation time of S9 segmentectomy was significantly longer than that of S9b subsegmentectomy ( $P < 0.01$ ). The median intraoperative blood loss was 50 ml (range, 35-230 ml). The median duration of chest tube insertion was 2 days (range, 1-4 days) and median length of postoperative hospital stay was 4 days (range, 3-7 days). No postoperative morbidity was identified. No perioperative death was identified. No recurrence or mortality was observed during the median follow-up period of 13 months (range, 1-34 months). The operative results of the patients are shown in (Table 2).

**Table 1:** Baseline characteristics of the patients.

Characteristic		
Age, years	Range	26-71
	Median	57
Male/female, n		5/12
Active smokers, n		2
BMI, kg/m <sup>2</sup>	Range	20.2-25.1
	Median	22.7
Image characteristics		
Size, mm	Range	8-17
	Median	13.7
Pure GGO, n		7
GGO with <50% solid part, n		10
Surgical resection margin, mm	Range	20.0-27.7
	Median	21.7

**Table 2:** Surgical types and perioperative outcomes.

Variables	n
<b>Surgical types</b>	
Right	8
RS9 segmentectomy	5
RS9b subsegmentectomy	3
Left	9
LS9 segmentectomy	7
LS9b subsegmentectomy	2
<b>Operative time, min RS9 segmentectomy</b>	
Range	75-217
Median	156
<b>LS9 segmentectomy</b>	
Range	67-171
Median	122
<b>S9 segmentectomy</b>	
Range	79-217
Median	167
<b>S9b subsegmentectomy</b>	
Range	67-131
Median	101
<b>Bleeding, ml</b>	
Range	35-230
Median	50
<b>Chest tube duration, d</b>	
Range	1-4
Median	2
<b>Postoperative hospital stay, d</b>	
Range	3-7
Median	4
Conversion to thoracotomy	0
Conversion to lobectomy	0
Postoperative complications	0
<b>Histologic subtypes</b>	
Invasive AC	7
MIA	7
AIS	2
AAH	1
<b>Pathological TNM stage of lung cancer (16 cases)</b>	
0	2
IA1	8
IA2	6
IA3	0

Ac: Adenocarcinoma; Mia: Minimally Invasive Adenocarcinoma; Ais: Adenocarcinoma In Situ; Aah: Atypical Adenomatous Hyperplasia. The operation time of left and right S9 segmentectomy was compared ( $P < 0.01$ ). The operation time of S9 segmentectomy and S9b subsegmentectomy was compared ( $P < 0.01$ ).

## Discussion

The bronchovascular pattern of the basal segments is the most complex [12]. The branching patterns of the left basal segmental bronchus are B8 and B9+10 at a frequency of 80%; B8+9 and B10 at 4%; and B8, B9, and B10 at 16%. When S\* is present (4% in frequency), care should be taken when distinguishing A10 and A\* from B10a and B\*. While the pulmonary artery usually branches into A8 and A9+10 at a frequency of 74%; into A8+9 and A10 at a frequency of 16%; and into A8, A9, and A10 at a frequency of 10%. The branching patterns of the left basal vein are V8+9 and V9+10 at a frequency of 30%; V8+9+10 and V10 at 6%; V8 and V8+9+10 at 4%; V8+9 and V10 at 28%; V8 and V9+10 at 24%; and V8, V9, and V10 at 8% [13]. The bronchovascular pattern of the right basal segments (S7, S8, S9, and S10) was more complex, the branching patterns of segmental bronchus are B8 and B9+10 at frequency of 86%, B8+9 and B10 at 8%, and B8, B9, and B10 at 6%. While the pulmonary artery usually branches into the A8 and A9+10 at a frequency of 90%, into A8+9 and A10 at a frequency of 8%, and into A8, A9, and A10 at a frequency of 2%. The branching patterns of right basal vein are V8+9 and V9+10 at a frequency of 30%, V8+9+10 and V10 at 14%, V8 and V8+9+10 at 2%, V8+9 and V10 at 26%, V8 and V9+10 at 18%, and V8, V9, and V10 at 10% [13]. Thoracoscopic segmentectomy for every basal segment is a technically challenging anatomical segmentectomy, with S9 segmentectomy being one of the most complex [9]. There are three methods that can be used. First is the interlobar fissure approach using an intersegmental tunneling to separate the superior segment (S6) and basal segments, wherein we can first expose the segmental hilum, thus exposing the pulmonary artery and bronchus branches and then resect the lateral part of the basal segment [14]. However, dividing the lung parenchyma and creating the tunnel were technique-demanding procedures, especially when the interlobar fissures were not complete. There is also concern regarding the possible torsion of S6 after complete separation from other segments. Second is the inferior lung ligament approach used to track the intersegmental plane following the inferior pulmonary ligament, which is considered a landmark for intersegmental division. This approach is reasonable, however, such a unidirectional dissection sometimes leads the surgeon to misunderstanding the anatomy if the surgeon does not have sufficient experience. Zhu and colleagues have reported a case of RS9 segmentectomy via inferior lung ligament approach [15], this surgical method was suitable for both left S9 segmental resection and right S9 segmental resection. To make the operation easier, we performed a 3D reconstruction to identify the branches of the pulmonary vessels of the patient [14,16]. Our results showed that the operation time of RS9 segmentectomy was significantly longer than that of LS9 segmentectomy ( $P < 0.01$ ), which may be related to the difference of bilateral anatomical structure, the bronchovascular pattern of the right basal segments was more complex. S9 consists of S9a and S9b. S9a is closer to the oblique fissure, while S9b is deeper. According to our experience, some S9 extends to oblique fissure, and some S9 does not extend to oblique fissure. B9b and A9b is more comfortable to take since they are located in the shallow and more accessible hilar structures from this approach. B9a and A9a are less accessible as their location are much deep. So, the operation time of S9 segmentectomy was significantly longer than that of S9b subsegmentectomy ( $P < 0.01$ ). Third is the bidirectional approach, which regards the pulmonary artery as the primary

landmark [6]. If the fissure is incomplete or inflammatory, this step can be tedious. Opening the fissure can lead to pulmonary tears and troublesome oozing. We prefer the inferior lung ligament approach, with the aid of 3D reconstruction, it is possible to accomplish all cases of S9 segmentectomy through an inferior pulmonary ligament approach, which is the preferred approach in our practice, without worrying about the fissures [8], the minimal range of surgical resection can be determined by setting the safe margin through three-dimensional reconstruction, and the operation mode (S9 segmentectomy or S9b subsegmentectomy) can be determined before operation. Tracking the target segmental branches by 3D reconstruction images during a single-direction thoracoscopic S9 segmentectomy starting from the inferior pulmonary ligament. In this approach, dissection proceeds from the pulmonary ligament to the hilum using the intersegmental septum as a landmark. We first encountered the inferior pulmonary vein, which has the most variations and combinations. From this point of view, the lack of a reference and insufficient surgical experience and anatomical knowledge may lead to miscalculation in identifying the vein branches. The accurate establishment of the target vein is challenging and should be overcome in S9 resection through the inferior lung ligament approach. In this situation, we have to expose pulmonary vein from proximal to distal side as possible by cutting lung parenchyma along intersegmental plane. Here we suggest that three-dimensional reconstruction should be introduced into the operation, given that it is a good tool to confirm the target segment vein and the intersegmental vein. Similarly, 3D reconstruction can help in tracking the target bronchi and reducing unnecessary exploration. We do not need to expose all the branches of the artery because it does not affect the accurate identification of the target artery. The artery generally corresponds to the bronchus one by one and slightly deviates from the spine. Of course, we can confirm A9 through 3D reconstruction.

Tailoring the intersegmental plane is another challenge encountered in VATS S9 segmentectomy. The anatomical characteristics of this segment make it difficult to imagine how multiple staplers tailor the segment. It starts from a relatively thin part of the lung tissue and gradually reaches the segmental hilum and the thick part of the lung, from the periphery to the center with “step-by-step” stapling [18]. The guidance of 3D reconstructed images not only enables to achieve a safe surgical margin but also minimizes the anatomic resection of lung tissues [19].

### Conclusions

The optimal surgical techniques and approach of thoracoscopic S9 segmentectomy remains the subject of debate, based on 3D interactive quantitative surgical planning, thoracoscopic S9 segmentectomy can be successfully performed using an inferior pulmonary ligament approach. 3D reconstruction is helpful for the surgeon to decide which segment should be resected and to know the anatomic features of the target segmental structures and its neighbors. We believe that even an inexperienced surgeon using 3D reconstruction can perform thoracoscopic S9 segmentectomy with acceptable safety and complications.

### Limitations

This study is a retrospective one without comparisons of techniques. However, because the experience with thoracoscopic S9 segmentectomy is still lacking worldwide, we believe that it is still

of importance to provide an additional option for thoracic surgeons to consider. The follow-up period of patients with lung cancer was short and long-term outcomes were expected.

### Declarations

**Author contributions:** Conception, study design and protocol: Y Liu, SL Zhang, CB Liu. Identification of studies: Y Liu, SL Zhang. Data analysis and interpretation: Y Liu; Manuscript writing: Y Liu. Project oversight and supervision: SL Zhang, CB Liu. Critical revisions for important intellectual content: All authors. All authors read and approved the final manuscript.

**Funding:** This work was supported by the Medical and Health Research Program (A20-2-015), Science & Technology Bureau of Yichang.

**Conflict of interest:** None declared.

### References

1. Handa Y, Tsutani Y, Mimae T, Miyata Y, Okada M. Complex segmentectomy in the treatment of stage IA non-small-cell lung cancer. *Eur J Cardiothorac Surg* 2020; 57: 114-21.
2. Wisnivesky JP, Henschke CI, Swanson S, Yankelevitz DF, Zulueta J, Marcus S. Limited resection for the treatment of patients with stage IA lung cancer. *Ann Surg* 2010; 251:550-4.
3. Shapiro M, Weiser TS, Wisnivesky JP, Chin C, Arustamyan M, Swanson SJ et al. Thoracoscopic segmentectomy compares favorably with thoracoscopic lobectomy for patients with small stage I lung cancer *J Thorac Cardiovasc Surg*. 2009; 137: 1388-93.
4. Yan TD. Surgical atlas of thoracoscopic lobectomy and segmentectomy. *Annals of Cardiothoracic Surgery* 2014; 3: 183-91.
5. Liu C, Liao H, Guo C, Pu Q, Mei J, Liu L. Single-direction thoracoscopic basal segmentectomy. *J Thorac Cardiovasc Surg* 2020; 160: 1586-94.
6. Sato M, Murayama T, Nakajima J. Thoracoscopic stapler-based “bidirectional” segmentectomy for posterior basal segment (S10) and its variants. *J Thorac Dis* 2018; 10: 1179-86.
7. Endoh M, Oizumi H, Kato H, Suzuki J, Watarai H, Masaoka T et al. Posterior approach to thoracoscopic pulmonary segmentectomy of the dorsal basal segment: a single-institute retrospective review. *J Thorac Cardiovasc Surg* 2017; 154: 1432-9.
8. Pu Q, Liu C, Guo C, Mei J, Liu L. Stem-Branch: a novel method for tracking the anatomy during thoracoscopic S9-10 segmentectomy. *Ann Thorac Surg* 2019; 108: 333-5.
9. Oizumi H, Endoh M, Takeda SI, Suzuki J, Fukaya K, Sadahiro M et al. Anatomical lung segmentectomy simulated by computed tomographic angiography. *Ann Thorac Surg* 2010; 90: 1382-3.
10. Nakamoto K, Omori K, Nezu K. Superselective segmentectomy for deep and small pulmonary nodule under the guidance of three-dimensional reconstructed computed tomographic angiography *Ann Thorac Surg*. 2010; 89: 877-84.
11. Wang J, Xu X, Wen W, Wu W, Zhu Q, Chen L et al. Modified method for distinguishing the intersegmental border for lung segmentectomy. *J Thorac Cancer* 2018; 9: 330-3.
12. Nagashima T, Shimizu K, Ohtaki Y, Obayashi K, Nakazawa S, Mogi A et al. Analysis of variation in bronchovascular pattern of the right middle and lower lobes of the lung using three-dimensional CT an-

- 
- giography and bronchography. *Gen Thorac Cardiovasc Surg* 2017; 65: 343-9.
13. Nomori H, Okada M. *Illustrated anatomical segmentectomy for lung cancer*. Heidelberg: Springer Science & Business Media; 2012.
  14. Igai H, Kamiyoshihara M, Kawatani N, Ibe T. Thoracoscopic lateral and posterior basal (S9 + 10) segmentectomy using intersegmental tunnelling. *Eur J Cardiothorac Surg* 2017; 51: 790-1.
  15. Zhu Y, Pu Q, Liu L. Trans-inferior-pulmonary-ligament single direction thoracoscopic RS9 segmentectomy: application of stem-branch method for tracking anatomy. *Ann Surg Oncol* 2020; 27: 3092-3.
  16. Kikkawa T, Kanzaki M, Isaka T, Onuki T. Complete thoracoscopic S9 or S10 segmentectomy through a pulmonary ligament approach. *J Thorac Cardiovasc Surg* 2015; 149: 937-9.
  17. Oizumi H, Kanauchi N, Kato H, Tndoh M, Suzuki J, Fukaya K et al. Anatomic thoracoscopic pulmonary segmentectomy under 3-dimensional multidetector computed tomography simulation: a report of 52 consecutive cases. *J Thorac Cardiovasc Surg* 2011; 141: 678-82.
  18. Zhu Y, Pu Q, Liu L. Trans-inferior pulmonary-ligament VATS basal segmentectomy: application of single-direction strategy in segmentectomy of left S9+10. *J Thorac Dis* 2018; 10: 6266-8.
  19. Wu WB, Xu XF, Wen W, Xu J, Zhu Q, Pan XL et al. Three-dimensional computed tomography bronchography and angiography in the preoperative evaluation of thoracoscopic segmentectomy and subsegmentectomy. *J Thorac Dis* 2016; 8: 710-5.